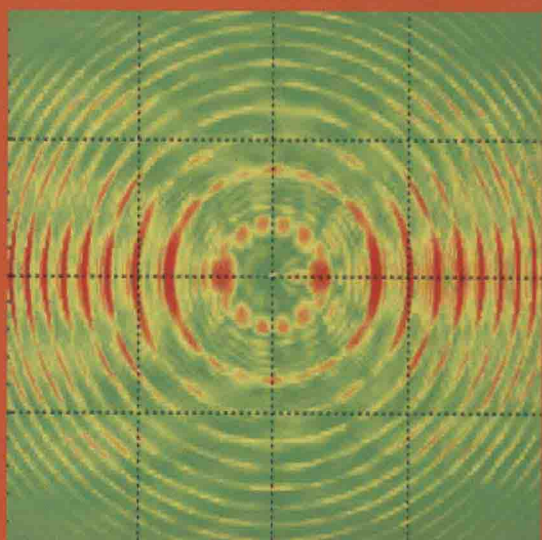
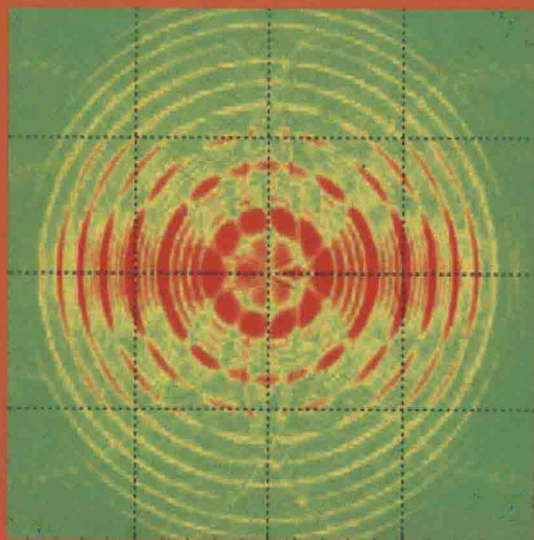
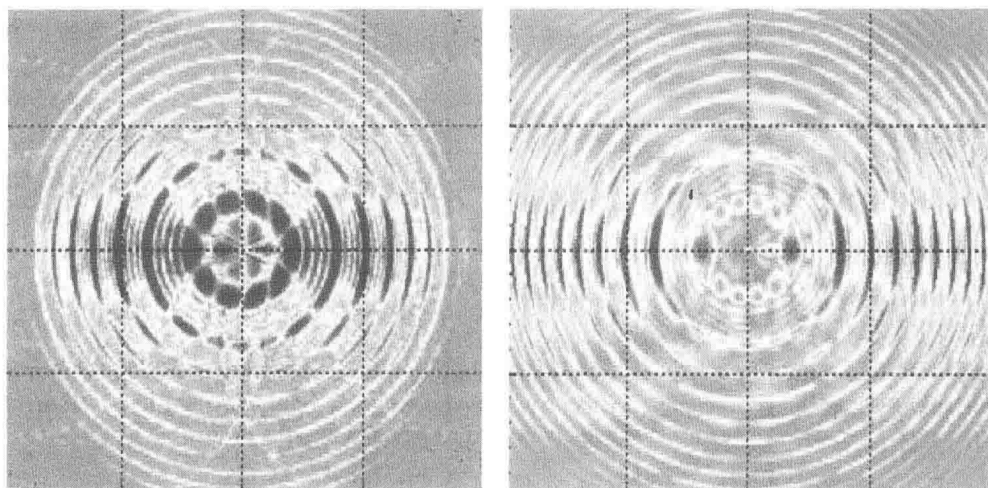


Advances of
Atoms and Molecules
in Strong Laser Fields



Yunquan Liu

Advances of Atoms and Molecules in Strong Laser Fields



Yunquan Liu

Peking University, China

 **World Scientific**

NEW JERSEY • LONDON • SINGAPORE • BEIJING • SHANGHAI • HONG KONG • TAIPEI • CHENNAI • TOKYO

Published by

World Scientific Publishing Co. Pte. Ltd.

5 Toh Tuck Link, Singapore 596224

USA office: 27 Warren Street, Suite 401-402, Hackensack, NJ 07601

UK office: 57 Shelton Street, Covent Garden, London WC2H 9HE

British Library Cataloguing-in-Publication Data

A catalogue record for this book is available from the British Library.

ADVANCES OF ATOMS AND MOLECULES IN STRONG LASER FIELDS

Copyright © 2016 by World Scientific Publishing Co. Pte. Ltd.

All rights reserved. This book, or parts thereof, may not be reproduced in any form or by any means, electronic or mechanical, including photocopying, recording or any information storage and retrieval system now known or to be invented, without written permission from the publisher.

For photocopying of material in this volume, please pay a copying fee through the Copyright Clearance Center, Inc., 222 Rosewood Drive, Danvers, MA 01923, USA. In this case permission to photocopy is not required from the publisher.

ISBN 978-981-4696-38-8

In-house Editor: Song Yu

Typeset by Stallion Press

Email: enquiries@stallionpress.com

Printed in Singapore

Preface

In parallel to the invention of first ultrashort laser in the mid-sixties, the field of research “atoms and molecules in strong laser fields” has evolved considerably during the last two decades owing to the rapid technological development of lasers as well as the advanced experimental techniques. Recent developments have shown that high intensity lasers open the way to realize pulses with the shortest durations to date, giving birth to the field of attosecond science ($1 \text{ asec} = 10^{-18} \text{ s}$). Irradiating atomic or molecular targets by an intense laser field leads to many highly nonlinear phenomena. “Atoms and molecules in strong laser fields” is a fascinating field in atomic, molecular and optical (AMO) physics, and it has progressed considerably during the last decade. In view of the rapid achievement in both experimental and theoretical studies of atoms and molecules in strong laser fields, it would now be very desirable to present a more comprehensive and advanced reviews text which contains all the new and important progress.

Depending on the laser wavelength and laser intensity, atomic and molecular physics in strong laser fields is essentially different. At near-infrared and visual wavelength where the commercial Ti:sapphire femtosecond lasers cover, multiphoton ionization and tunneling ionization usually dominates. On the other hand, the Free Electron Laser (FEL) facilities, emerging as a rapid developing technology in advanced light sources in the last decade, provides the coherent, brilliant and ultrashort light pulse which, is tunable from Terahertz to X-ray regime, and now opens up new vistas in the study of the atomic and molecular physics.

This book is about recent progress of atoms and molecules in strong laser fields. The goal is to give an up-to-date introduction to the broad range of strong-field AMO (atomic molecular and optical) physics, i.e., tunneling ionization, multiphoton ionization, photoelectron holography, electron correlation, controlling molecular dissociation, high harmonic generation, attosecond science, and X-FEL laser physics, etc. As an expanding field, a lot of intriguing progress has been achieved. It is ‘no way’ to collect all of them. It is expected that there will be a lot of activities in this research area in the near future.

I would like to take this opportunity to thank all the authors for their important contributions. It is hoped that this collection will be useful not only to active researchers in the strong-field community but also to other scientists in biology and chemistry.

Yunquan Liu
Peking University

Contents

<i>Preface</i>	v
1. Long Range Ionic Potential Effect on Strong-Field Tunneling	1
<i>Xufei Sun, Min Li, Chengyin Wu, Yunquan Liu</i>	
1 Introduction	1
2 Experimental Technique	4
3 Low Energy Structure	5
4 Local Ionization Suppression	8
5 Coulomb Asymmetry	14
6 Conclusion	20
Acknowledgment	20
References	20
2. Photoelectron Interference and Photoelectron Holography	25
<i>Min Li, Qihuang Gong, and Yunquan Liu</i>	
1 Introduction	25
2 Semiclassical Model with Implementing Interference Effect	27
2.1 Intercycle interference and intracycle interference	27
2.2 Forward rescattering photoelectron interference	29
2.3 Backward rescattering photoelectron interference	31
3 Classical-Quantum Correspondence of above Threshold Ionization	38
4 Conclusion	48
References	48

3. Dissociation of Hydrogen Molecular Ions in Strong Laser Fields	51
<i>Feng He</i>	
1. Introduction	51
2. Numerical Methods	52
3. Dissociation in Strong Laser Fields	55
A Electron localization	56
B Dissociation in long wavelengths and short wavelengths	59
C Dissociation in short and intense laser fields	64
D Control vibrational states	67
E Rescattering dissociation	70
F Two dimensional wave packet propagation	74
Conclusion	76
Acknowledgment	77
References	77
4. Nonsequential Double Ionization of Atoms in Strong Laser Field	81
<i>Difa Ye, Libin Fu and Jie Liu</i>	
1 Introduction	82
2 Semiclassical Model	83
3 The Surprising Fingerlike Structure in NSDI	84
4 NSDI Below the Recollision Threshold	90
5 Atomic Species Dependence of NSDI	100
Acknowledgment	109
References	109
5. Few-Photon Double Ionization of He and H ₂	111
<i>Wei-Chao Jiang, Wei-Hao Xiong, Ji-Wei Geng, Qihuang Gong, and Liang-You Peng</i>	
1 Introduction	111
2 Numerical Implementation to Solve Two-Electron TDSE	112
2.1 General technologies in solving TDSE	112
2.1.1 Time-propagation method	113
2.1.2 Space discretization method	115

2.2	Methods to solve TDSE of helium	118
2.2.1	Time-dependent close coupling (TDCC) scheme	118
2.2.2	Extraction of physical observables	120
2.3	Methods to solve TDSE of H ₂ molecule	122
2.3.1	Introduction of the prolate spheroidal coordinates	122
2.3.2	TDSE of H ₂ molecule in the prolate spheroidal coordinates	123
2.3.3	Extraction of physical observable	128
3	Applications of TDSE Methods on Double Ionization Processes	129
3.1	One-photon and two-photon double ionization cross sections	129
3.1.1	Definitions for photon-double ionization cross sections	129
3.1.2	Numerical results for electron spectrums of helium atom and H ₂ molecule	131
3.1.3	Recoil ion spectrum of photon double ionization of helium	136
3.2	Electron correlation in the joint angular distributions	141
3.3	Double ionization of helium by double attosecond pulses	146
	References	151
6.	Probing Orbital Symmetry of Molecules Via Alignment-Dependent Ionization Probability and High-Order Harmonic Generation by Intense Lasers	157
	<i>Song-Feng Zhao, Xiao-Xin Zhou and C. D. Lin</i>	
1	Introduction	158
2	Theoretical Methods	160
2.1	Construction of one-electron potentials of linear molecules	160
2.2	Calculation of molecular wavefunction with correct asymptotic tail by solving the time-independent Schrödinger equation	162
2.3	The MO-ADK and MO-PPT models	164

2.4	Calculation of the orientation-dependent ionization probability of molecules with the MO-SFA model	166
2.5	The molecular Lewenstein model for HHG from molecules	166
3	Results and Discussions	167
3.1	The one-electron potentials for Cl_2	167
3.2	Extracting structure parameters for several highly occupied orbitals of linear molecules	167
3.3	Comparison of alignment dependent ionization probabilities between the MO-ADK model and other more elaborate calculations	169
3.4	Comparison with experiments	171
3.5	Alignment dependence of ionization rates from HOMO, HOMO-1, and HOMO-2 orbitals	171
3.6	Probing the shape of the ionizing molecular orbitals with the orientation-dependent ionization rates	172
3.7	Examination of the validity of the MO-ADK and MO-PPT models	173
3.8	Probing the molecular orbital with the alignment-dependent HHG signals	175
4	Conclusions	178
	Acknowledgments	179
	References	179
7.	High-order Harmonic Generation Driven by Sub-Cycle Shaped Laser Field	185
	<i>Yinghui Zheng, Zhinan Zeng, Pengfei Wei, Jing Miao, Ruxin Li, and Zhizhan Xu</i>	
1	Introduction	185
2.1	Two pulses scheme	187
2.2	Multi-color field scheme	191
	Acknowledgment	201
	References	201
8.	Imaging Ultra-fast Molecular Dynamics in Free Electron Laser Field	205
	<i>Y. Z. Zhang and Y. H. Jiang</i>	
1.	Introduction	205
2.	The Temporal Characteristic and Resolution of Free Electron Laser	209

3. The EUV Pump/Probe Measurement	212
3.1. The split-mirror scheme	212
3.2. Tracing the nuclear wave-packet in D_2^+ by EUV time-resolved experiment	213
3.3. Nuclear wavepacket dynamics in excited states of N_2	215
3.4. Ultrafast photoisomerization of acetylene cation	217
3.5. Time-resolved interatomic Coulombic decay (ICD) in Ne_2	218
3.6. Electron rearrangement dynamics in dissociating I_2^{n+}	221
4. Optical-pump — X-ray-probe (OPXP) Experiments	222
4.1. Probing a prototypical photoinduced ring opening	223
4.2. Imaging charge transfer in iodomethane	225
5. Summary and Outlook	228
Acknowledgments	230
References	230

Chapter 1

Long Range Ionic Potential Effect on Strong-Field Tunneling

Xufei Sun, Min Li, Chengyin Wu, Yunquan Liu

*Department of Physics and State Key Laboratory for Mesoscopic Physics,
Peking University, Beijing 100871, China
yunquan.liu@pku.edu.cn*

The tunneling ionization as one of the fundamental quantum processes exposing of atoms in strong laser fields, has been investigated intensively in recent decades. The tunneling ionization has intrigued many important implications. As the first stage, the post ionization effects have been revealed in high-resolution experiments. All of those experiments indicate the importance of the long range potential on the tunneling ionization. In this chapter, we will overview the long-range potential effect on strong-field tunneling. Especially, the long range ionic potential has significant effect on the low-energy photoelectron energy structures (“ionization surprise”), the ionization asymmetry and the local ionization suppression.

1. Introduction

The pioneering theoretical description of the photoionization of atoms and ions exposed to high-intensity laser radiation is underlain by the Keldysh theory proposed in 1964 [1]. The ionization potential I_p of an atom is defined as the energy required to lift its most loosely bound electron into the continuum (a bound-continuum transition). When irradiated by light of sufficiently high frequency ω , this is possible via a single-photon transition [2]. If increasing the laser intensity ionization is also possible in lower frequency fields. Here, ionization takes place via the absorption of n photons of energy $\hbar\omega$, such that $(n - 1)\hbar\omega < I_p < n\hbar\omega$. The corresponding multiphoton ionization rate can be obtained by treating the field as a small perturbation with respect to the Coulomb potential of the atom [3, 4].

The associated theoretical framework is called lowest order perturbation theory and results in an intensity scaling that takes the form of a power law. However, with increasing intensity, higher order terms become significant requiring an extension of perturbative theory.

Above-threshold ionization (ATI), as one of the cornerstones in strong-field community, has attracted an abundance of attention. This intriguing phenomenon is characterized by a series of peaks separated by the laser frequency in the electron energy spectrum and the relative yield of each peak drops exponentially with increasing the electron energy. Beyond that, a photoelectron plateau structure with an approximately constant amplitude is discovered from $\sim 2U_p$ extending up to an abrupt cutoff at around $10U_p$ [U_p is the ponderomotive energy, $U_p = F^2/4\omega^2$, where F and ω are the laser field strength and laser frequency, respectively. Atomic units (a.u.) are used throughout unless specified] [5].

Alternatively, increasing the laser intensity, the potential barrier of an atom is suppressed drastically and electrons can easily escape from the atom through tunneling, as seen in Fig. 1. Usually, multiphoton ionization and tunneling ionization are distinguished by the Keldysh parameter γ [6] ($\gamma = \sqrt{2I_p/U_p}$, I_p : the ionization potential). Tunneling ionization will dominate if $\gamma < 1$, while multiphoton ionization prevails when $\gamma > 1$.

A thorough understanding of atomic ionization in strong fields is essential for further explorations and diverse applications. Electron tunneling is a key process when atoms and molecules are exposed to strong laser fields. Strong-field tunneling ionization has triggered a rich set of physical phenomena that are closely associated with the flourishing attosecond physics. Strong laser field ionization now provides a sophisticated method to image and probe the atomic and molecular quantum processes. Recent advances in strong field physics have opened a window to precisely measure the delay time and the initial coordinates of quantum tunneling [7, 8].

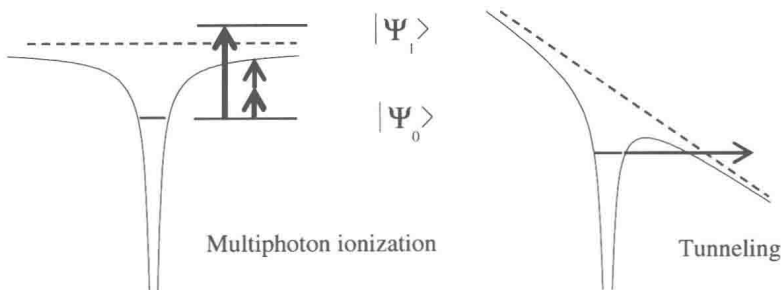


Fig. 1. The illustration of multiphoton ionization and tunneling ionization when atoms with a ionization potential of I_p in strong laser fields.

For the case of linearly polarized light the motion of atomic or molecular fragments emerging from ionization can be naturally separated into a longitudinal part, which is parallel to the electric field polarization, and a part transverse to the field. Under these assumptions analytical expressions for the final momentum distributions along longitudinal direction $w(p_{\parallel})$ and perpendicular or transverse' directions $w(p_{\perp})$ to the field polarization were obtained [9]:

$$w(p_{\parallel}) \propto \exp\left(-\frac{p_{\parallel}^2 \omega^2 (2I_p)^{3/2}}{3E^3}\right)$$

$$w(p_{\perp}) \propto \exp\left(-\frac{p_{\perp}^2 (2I_p)^{1/2}}{E}\right)$$

The Simple-man model is very fundamental for the understanding on strong-field ionization. In this model, strong-field ionization takes place in two-step, e.g., the electron is initially released through tunnelling and then classically propagates in the laser field. During the propagation process, the influence of the atomic potential is neglected. This model was later improved by taking into account of recollision effect (three-step Simple-man model) [10, 11]. In this three-step model, the tunnelled electron is accelerated in the laser field, then changes its travelling direction and finally is scattered upon the nucleus, giving rise to high-order above-threshold ionization (HATI) for elastic scattering with $10Up$ cut off [12], nonsequential double ionization (NSDI) for inelastic scattering [13] and high-harmonic generation (HHG) for recombination [14].

According to the Simple-man model, the electrons released at different tunnelling phase can be clarified into direct electrons and rescattered electrons in each half laser cycle. The electron tunnelled before the laser maximum will be directly pulled away by the laser field, so those electrons are termed as “direct electrons”. Alternatively, the electrons released after the laser maximum will be scattered by the nucleus one or several times and they are termed as “rescattered electrons”. As the basic processes, electron direct tunneling and rescattering lie in the very heart of attosecond physics [15, 16]. Both direct tunneling and rescattering effects have been successfully used to resolve molecular orbitals [17, 18].

Many strong-field phenomena appearing in atomic and molecular ionization by intense laser fields are explained within the framework of the strong-field approximation (SFA). In this approximation, the motion of an electron after ionization is assumed to be influenced by the electric field of the laser pulse only. The Coulomb field of the ionized atom is neglected as it quickly decreases with increasing distance of the electron from the ion. If considering the long-range Coulomb potential, the electron classical motion will be modified, as shown in Fig. 2. Once the electron is set free at the tunnel exit, its motion is dominated

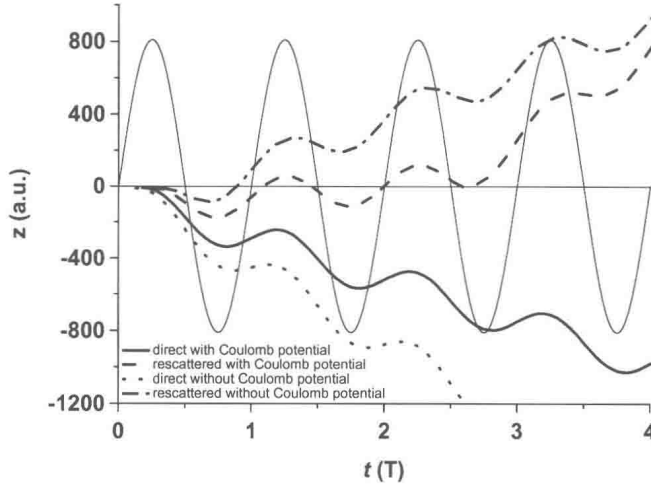


Fig. 2. The electron trajectories of direct electrons and rescattered electrons with and without considering the long-range Coulomb potential.

by the interaction with the laser field even though modified by the long-range ionic Coulomb potential, which both may lead to various photoionization effects. In this chapter, we will review the recent progress on the long range Coulomb potential on the tunnelling ionization, which benefits from the recent high-resolution experimental efforts.

2. Experimental Technique

All the experimental results presented in this chapter were measured with the combination of a strong laser system and a state-of-art technique in atomic physics, i.e., cold-target recoil ion momentum spectroscopy (COLTRIMS) [19]. In the experiments, we employed the 25 fs, 795 nm pulses from a Ti:Sa laser system with 3 kHz repetition rate, amplified pulse energy up to 0.8 mJ. In this amplified laser system, the initial pulses of ~ 4 nJ energy and 12 fs duration were delivered by a broadband Kerr-lense mode-locked Ti:Sa oscillator with 75 MHz repetition rate. The air and material dispersion was controlled by a set of dispersive mirrors. The pulses were amplified with the so-called ‘chirped-pulse amplification’ technique [20], i.e., they were stretched to 6–7 ps in a 10 mm thick glass block before being sent to a multipass amplifier system. Stretching was needed in order to reduce the peak intensity of the pulse and, thus, to stay below the damage threshold of the amplifier crystal. The beam passed 9 times through the amplification medium (Ti:Sa crystal pumped by a 3 kHz Nd:YAG laser of 5–6 mJ pulse energy and ~ 160 ns duration). After the fourth path the repetition rate was reduced from 75 MHz to 3 kHz by means of a Pockels cell. Due to the gain profile of the crystal, the spectrum of the amplified

pulses was narrowed to ~ 70 nm FWHM. The dispersion introduced by a glass block as well as by the other optical elements was compensated by a prism compressor. In addition, in order to compensate the third-order dispersion of the whole laser system, so-called TOD ('third-order dispersion') mirrors were introduced in the oscillator region. The wavelength acceptance of the compressor further reduced the pulse spectral width to ~ 40 nm FWHM, resulting in the production of Fourier-limited 25 fs (FWHM) pulse with a central wavelength of ~ 790 nm and a pulse energy up to $800 \mu\text{J}$.

Along with the impressive advances in femtosecond laser technology, within last 20 years tremendous progress has been achieved in the development of novel multi-particle detection techniques for atomic and molecular physics. This culminated in the realization of the so-called 'reaction microscopes', which were nicknamed as 'bubble chambers of atomic and molecular physics'. These machines, based on a combination of COLTRIMS and novel photoelectron imaging spectrometers, enable coincident measurements of several charged reaction fragments (ions and electrons) with excellent momentum and energy resolution, and with detection solid angle close to 4π . Often so-called 'kinematically complete' experiments, where full three-dimensional momentum vectors of all final-state reaction products are determined, become feasible. The main results presented in this chapter, were obtained with a reaction microscope with photoelectron momentum resolution ~ 0.05 a.u. (atomic units) along the time-of-flight direction and ~ 0.08 a.u. along the transverse direction. The electric (~ 5 V/cm) and magnetic (~ 8 G) fields were applied along the time-of-flight axis. Ions and electrons were measured with two position-sensitive microchannel plate (MCP) detectors respectively. From the time-of-flight and position on the detectors, the full momentum vectors of particles were calculated. In the off-line analysis, the photoelectrons were selected in coincidence with their singly charged parent atomic ions.

3. Low Energy Structure

Recently, high-resolution experiments on above threshold ionization [21] provided evidences for the resonant origin of detailed narrow structures within the plateau, in agreement with a series of numerical simulations [22–24]. A comprehensive numerical analysis of the problem [25] revealed a close relation between the resonant-like behaviour within the plateau and the existence of electron trajectories which lead to multiple recollisions with the parent ion ([26]). The significance of multiphoton resonances for "super-ponderomotive" photoelectrons in the tunnelling regime was predicted for the case of He [27], but until now was not confirmed experimentally.

The new phenomenon, dubbed as “ionization surprise” [28, 29] that in the tunnel regime an unexpected structure in the electron-energy spectrum was observed at small energies, which could not be explained within the SFA but could be seen in full quantum mechanical [30, 31] and also classical calculations [31, 32]. First high-resolution measurements on single ionization clearly demonstrated deviations from the smooth Gaussian shape, manifested as a small deep at zero in the electron (and, thus, ion) momentum distribution parallel to the laser polarization for Ne [33]. For the case of He this was predicted within the semiclassical model [34], where tunnelling with subsequent classical propagation of the emitted electron in the combined laser field and Coulomb field of the ion was considered. While for the case when Coulomb interaction was taken into account, a clear minimum is observed, the calculation for which the Coulomb interaction has been switched off yielded a smooth Gaussian-like curve. In the same work the authors predicted some deviations from the Gaussian shape also for the transverse momentum distribution.

Later, the origin of the low-energy structure (LES) [30, 31] was analyzed in detail and was shown to be a largely classical effect of the combined laser and Coulomb fields on the electronic motion after ionization. More recently, it was shown that the formation of the LES is due to a bunching or focusing of electrons during “soft recollisions” [16, 35]. At turning points of the quiver motion of the electron in the vicinity of the ionic core ($z \sim 0$ in combination with momentum $p_{\parallel} \sim 0$), In contrast to the prediction of the standard tunneling picture within the framework of strong-field approximation, it has been discovered that low-energy photoelectrons in the above threshold ionization process possess nontrivial behavior. For example, the momentum distribution of photoelectrons shows some intriguing low-energy structures, which deviated obviously from the Simpleman’s perspective. The low energy structure observed in the momentum distributions along the laser polarization has been intensively investigated recently and its mechanism is still in debate [36–41]. Semiclassical model has been applied to explore this low-energy structure and revealed the essential role of the long range Coulomb potential in its production.

In Figs. 3(a)–3(c), the low-energy part of the measured photoelectron spectra (collected in a solid angle of 5–8 degrees in the field direction) of noble gas atoms at different laser wavelengths and intensities are illustrated. The parameters chosen here guarantee that the process is in the tunneling regime ($\gamma < 1$). Several above threshold ionization peaks can be clearly seen in the spectrum for wavelength of 800 nm. With increasing wavelength, the ATI peaks become less pronounced and can be hardly distinguished in the spectrum for 1800 nm. On the other hand, the LES becomes noticeable in the long-wavelength spectra. It was denoted this as the high-energy low-energy structure (HLES), in order to distinguish it from the